Errors In Ambient Gas Concentration Measurement Caused By Acoustic Response Of Electrochemical Gas Sensors

Anna K. Farquhar[1*], Geoff S. Henshaw[1], David E. Williams[2]

1: Aeroqual Ltd, 460 Rosebank Road, Avondale, Auckland 1026, New Zealand

2: MacDiarmid Institute for Advanced Materials and Nanotechnology, School of Chemical Sciences, University of Auckland, Private Bag 92019, Auckland 1142, New Zealand

anna.farquhar@aeroqual.com geoff.henshaw@aeroqual.com david.williams@auckland.ac.nz

Abstract

Electrochemical sensors are used to measure electroactive gases in ambient air monitoring applications. These sensors typically contain sulfuric acid electrolyte, and porous carbon working, reference, and counter electrodes. Current fluctuations caused by fluctuations in the meniscus contact shape or area at the 3 phase gas-electrolyte-electrode interface as a result of ambient pressure fluctuations have been suggested as a potentially significant source of error in sensor measurements. We confirm in the present work that the pressure oscillations associated with ambient sound can indeed lead to significant signals. . We show, for a variety of commercial sensors for ambient nitrogen dioxide (NO_2), that acoustic noise equivalent to that from a nearby motorcycle or heavy goods vehicle can cause transient current fluctuations at 2 Hz sampling rate equivalent in the sensor output to as much as that due to 100 parts per billion by volume (ppb) of NO_2, and with a root mean square (RMS) variation averaged over 10s of approximately 40 ppb equivalent. These observations indicate that electrochemical gas sensors can behave as “microphones” in response to loud noise. The impact of acoustic noise should be considered when using electrochemical sensors to measure ambient air quality in areas of significant noise pollution, particularly if the aim is to resolve local transient concentration variations.

Keywords

Electrochemical sensors, acoustic stimulation, microphones, baseline current, ambient air quality, reliable data, Fourier transform, meniscus perturbation, three-phase contact line

Introduction

Electrochemical sensors are often used for the quantification of various electroactive gases. They typically contain a set of three porous electrodes, separated by thin, porous support membranes. A wicking material connects these planar electrodes to the electrolyte reservoir, upon which the electrode assembly sits. The working electrode is positioned at the top of this assembly, with a gas diffusion membrane separating the working electrode from the atmosphere to be sampled, forming a three-phase (gas-electrode-electrolyte) interface. Often, the electrodes are based on porous carbon materials and the electrolyte is sulfuric acid.[1, 2] Electroactive gases, including ozone, nitrogen dioxide and carbon monoxide, diffuse through the membrane and contact the working electrode at this three-phase interface where they undergo an oxidation or reduction reaction, generating a current that is proportional to the gas concentration in the sampled atmosphere. The electrode and electrolyte are designed so that the electrochemical reactions of the target gas at the working electrode are sufficiently fast and diffusion of the target gas through the gas diffusion membrane is the rate determining step[1]. In addition to the target gas reactions, there are baseline current reactions taking place at the working electrode, most likely oxygen reduction and electrode oxidation.[3] These result in a non-zero baseline current at the working electrode in the absence of target gas, caused by humidity dependent variations of the sulfuric acid concentration between the working and reference electrodes.[4, 5]

Electrochemical sensors have been explored as a low-cost method for measuring the concentration of critical pollutant gases in outdoor, typically urban, environments. Electrochemical gas sensors were originally developed for industrial health and safety monitoring, where concentrations are in parts-per-million by volume (ppm), however they have been shown to be useful in measuring parts-per-billion (ppb) levels in environmental monitoring.[6-8] Although designed to measure the

reduction or oxidation current of electroactive gases, there are several other processes occurring at the working electrode that influence sensor behaviour. Several authors have reported a persistent shift in the baseline current in response to changes in atmospheric temperature or relative humidity.[9-11] We have previously deduced that the temperature and humidity induced baseline current offset is caused by small changes in the potential determining reactions of the working and quasi-reference electrodes.[4] Additionally, a large amplitude signal fluctuation (± 10-20 ppb equivalent, frequency ≈ 0.001 Hz) has been reported, which correlates with fluctuations in relative humidity over short time scales.[12-14] In previous work we have demonstrated that the large amplitude fluctuations are primarily caused by fluctuations in relative humidity. Changes in relative humidity will cause fluctuations in the interfacial electrolyte composition and therefore fluctuations in the interfacial capacitance of the working electrode. Changes in interfacial capacitance lead to significant charging currents which manifest as large amplitude fluctuations in baseline current.[4]

Several authors have also observed a significant high frequency (0.0167 – 1Hz) noise component in the signal current in measurement in the urban atmosphere but not in the laboratory: eg [6, 15]. The response time of the sensors to step changes in gas concentration is on the scale of 10 s or less so it might be tempting to ascribe these fluctuations to rapid and large fluctuations in gas concentration in the vicinity of the sensor. Mead et al.[6] indicated that this high frequency noise correlated with periods of high wind speed. Weissert et al.[15] observed that this high frequency noise was related to the time of day, with increased noise in the middle of the day when acoustic noise from road traffic was highest. Sedlák et al.[16] explored the effect of flow rate on electrochemical gas sensors and showed that high frequency baseline current fluctuations depend on air flow rate across the sensor.

In a recent review, fluctuations in the baseline current were hypothesised as in part due to perturbations of the meniscus at the three-phase interface. The solid-liquid-gas contact line or meniscus for a porous carbon electrode has a complex shape with multiple possible configurations

and could switch between configurations in response to pressure fluctuations or to fluctuations in interfacial tension (caused for example by fluctuations in humidity).[2]. The baseline current of an electrochemical gas sensor is primarily due to oxygen reduction and electrode oxidation. These baseline reactions are not necessarily limited by diffusion and therefore their rate will depend on the working electrode area in contact with the electrolyte. Maget and Roethlein showed the effect of the meniscus on oxygen reduction at platinum electrodes [17]. Chan et al.[18] determined that changes in air pressure at the three-phase interface of copper electrodes in potassium hydroxide electrolyte caused changes in the meniscus contact angle, with a decrease in contact angle at increased pressure. The oxygen reduction current changed as a result of this contact angle change. More generally, fluctuations in meniscus shape cause fluctuations in the rate of redox reactions occurring within the meniscus because of the effect of the boundary on diffusion within the confined liquid [19, 20]. On electrodes covered with thin liquid films, such as are formed close to the meniscus, the current due to the oxygen reduction reaction is dominated by the part of the electrode that is very close to the gas-electrode-electrolyte 3-phase contact line [21].

Air pressure fluctuations could cause fluctuations in the meniscus shape within the porous electrode structure and hence on the current due to the oxygen reduction reaction. Two sources of high frequency pressure fluctuations are possible: acoustic noise and acoustic resonance (Helmholtz resonance). In the present work, we study the effect of acoustic noise on the baseline current of electrochemical sensors. We show that the RMS variation of the baseline current in response to loud sound increases with acoustic stimulation and the frequency of the baseline current fluctuations depend on the frequency of the applied sound wave. An electrochemical gas sensor therefore behaves as a “microphone” in response to changes in ambient sound. Whilst the effect may be averaged to zero over a sufficiently long time (eg 15 min – 1 hr) as in previous studies, the impact of acoustic noise stimulation of the baseline current of electrochemical gas sensors should be considered when using electrochemical gas sensors in areas with significant noise pollution, for

example next to a busy urban road, particularly if the aim is to resolve transient gas concentration changes.

Experimental

Laboratory Studies

An electrochemical gas sensor was positioned 5 cm from a speaker and subject to soundwaves of varying frequencies and volumes. For most experiments, an O_3M5 sensor (Membrapor AG, Switzerland) was used. To confirm reproducibility across sensor types and manufacturers, other sensors were also tested - NO_2-A1 (NO_2 and O_3, Alphasense UK) and CO-AX (CO, Alphasense UK). All experiments were carried out in laboratory air, where the concentration of NO_2 and O_3 are negligible. To confirm this, the current of an O_3M5 sensor was recorded in zero air (generated using an Aeroqual Aircal 1000) and compared with the current in laboratory air. As shown in SI Figure S2, the average current in zero air is the same as the average current in the laboratory air, within error. If NO_2 or O_3 were present, the current would be negative (for example 100 ppb of O_3 would cause an offset of -100 nA). Hence, we can assume the results presented are due to baseline current reactions (likely oxygen reduction and electrode oxidation), not target gas reactions. The O_3M5 sensor was positioned a fixed distance from the speaker (5 cm unless otherwise stated). The sensor was positioned such that the sensor membrane was directly facing the source of sound. The sound was generated using an online tone generator (https://www.szynalski.com/tone-generator/). Sound was generated at a single frequency with a volume of 100 dBA unless otherwise stated. For the mixed sound, three different frequencies (250, 350, and 450 Hz) were generated simultaneously. The frequency and decibel level of the sound was recorded using the Physics Toolbox Sensor Suite application on an Apple iPhone. The phone was positioned immediately next to the sensor to measure the frequency and decibel level experienced by the sensor. The baseline current was recorded using an EmStat Pico Development kit from PalmSens BV (Houten, Netherlands). Current was recorded using a 1 Hz or 1 kHz sampling frequency at 0 V vs. sensor quasi-reference electrode.

Field Studies

The O_3M5 sensor was operated in three different "real-world" settings: in a quiet office area, outdoors approximately 200 m from the nearest road, and outdoors next to Rosebank Road in Auckland, New Zealand – a busy road in a predominantly industrial area in Auckland. Current was collected using the EmStat Pico Development kit at a 2 Hz sampling frequency over a 5 minute period. The sound volume was recorded using an Apple iPhone and the Physics Toolbox Sensor Suite application. The road was visually monitored throughout the experiment, and any noise generating events (for example passing trucks) were recorded.

Results and Discussion

In this work we study the impact of acoustic noise on the baseline current of an electrochemical gas sensor. Sensors of this type measuring nitrogen dioxide(NO_2) in air respond have current response linear in gas concentration and typically have signal current of 1000 nA / ppm (part-per million by volume of the target gas in air) [1, 6, 15]. In a polluted urban atmosphere, NO_2 concentrations might typically be 100 ppb, corresponding to a signal current of 100 nA. Figure 1A shows the baseline current of an O_3M5 sensor with and without acoustic stimulation, sampled at 1 Hz. There is a clear increase in the amplitude of the baseline current fluctuations with acoustic stimulation, with an increase in the RMS variation of the time series data from 15 to 40 nA. Fluctuations of up to ± 100 nA (100 ppb equivalent) occur with acoustic stimulation. The result of measurement with a sampling frequency of 1 kHz (the maximum available with the EmStat Pico development kit) is given in Figure 1B. A clear increase in the high-frequency baseline noise can be seen with acoustic stimulation. The noise signal is symmetrical about zero. Figure 1C shows the baseline noise of the electrochemical sensor at a sampling frequency of 1 kHz at different distances from the speaker with 450 Hz acoustic stimulation. Moving the sensor further from the source of sound decreases the amplitude of the baseline noise. The impact of acoustic stimulation clearly depends on the proximity of the electrochemical sensor to the source of sound. In this experiment, only the electrochemical sensor

was moved, confirming this effect is due to the electrochemical sensor and not the electronic circuitry recording the sensor signal.

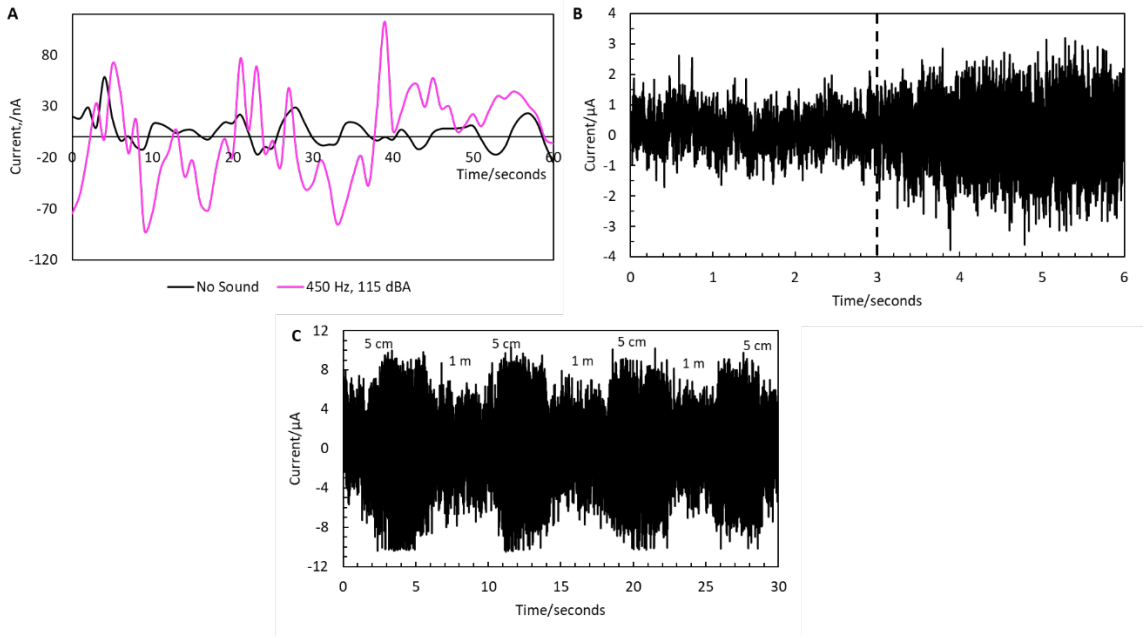

Figure 1: (A) Baseline current of an O_3M5 sensor with and without acoustic stimulation and a 1 Hz sampling rate. (B) Baseline current of an O_3M5 sensor with and without acoustic stimulation and a 1 kHz sampling rate. Dashed line indicates when the sound was applied. For (A) and (B) the sensor was 5 cm from the speaker. (C) Baseline current of an O_3M5 sensor 5 cm and then 1 m from the source of sound. Sound frequency for all experiments was 450 Hz and the volume at 5 cm was 100 dBA.

We hypothesize that this increase in the amplitude of the baseline current noise is due to perturbations of the meniscus at the three-phase contact line caused by air pressure fluctuations at the interface. Fluctuations in the meniscus will change the electrode surface area that is in contact with the electrolyte and therefore the oxygen reduction or electrode oxidation current. More subtly, fluctuations in the meniscus shape change the distance scale for diffusion of oxygen towards the electrode, particularly near to the contact line, and hence the current flowing there.

The influence of the frequency of the acoustic stimulation was investigated. Time series data, collected at 1 kHz, of the baseline current of an O_3M5 sensor stimulated by soundwaves of 250, 350 and 450 Hz (sound volume was fixed at 100 dBA), was processed via a discrete Fourier transform to determine the periodicity of the baseline noise with different acoustic stimulation frequencies and

the results are given in Figures 2B, C and D, while Figure 2A shows the Fourier transform of the baseline noise in the absence of sound. When the electrochemical sensor is stimulated with a soundwave of a fixed frequency, the baseline noise can be decomposed into a single constituent frequency. The constituent frequency of the baseline current signal shifts depending on the frequency of the applied soundwave; however, it is not the same as the frequency of the soundwave. For example, a 250 Hz soundwave gives an O_3M5 signal frequency of 320 Hz. Note that the frequency recorded using the Physics Toolbox application did match the applied sound frequency i.e. if a soundwave of 250 Hz was generated, the application recorded a frequency of 250 Hz. The baseline current was also recorded with a mixture of sound frequencies generated simultaneously and Fourier transform results are given in Figure 2E. The analysis shows the baseline current can be decomposed into three discrete frequencies. Furthermore, these frequencies match those obtained in the single frequency experiments.

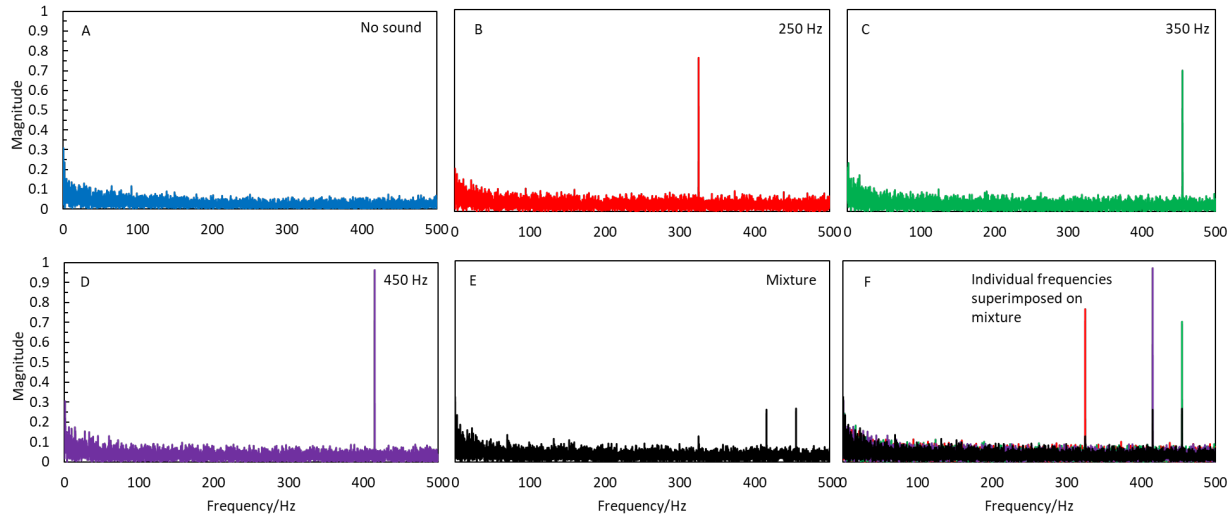

Figure 2: Fourier transform analysis of the baseline current of an O_3M5 sensor with (A) no sound; (B) a 250 Hz soundwave; (C) a 350 Hz soundwave; (D) a 450 Hz soundwave; (E) mixture of 250, 350, and 450 Hz sound waves. (F) shows the individual frequency experiments superimposed on the mixed frequency experiment. All experiments were carried out with the sensor 5 cm from the speaker and a volume of 100 dBA. The sampling rate was 1 kHz.

The mismatch of the applied and recorded frequency is most likely an aliasing artifact, which we confirmed by alteration of the sampling rate (SI, Figure S3). Aliasing artifacts result from under sampling and mean the reported frequency in the Fourier transform analysis does not necessarily

reflect the true frequency of the time series data. A description of aliasing artifacts can be found in the SI. Use of the maximum available sample rate of 1 kHz, used for the remainder of the frequency analysis, ensured reproducibility, but meant the frequency determined by the Fourier transform analysis does not necessarily represent the true frequency of the baseline current. Measurement of the amplitude of the response peak in the transform was a convenient way to separate the effect of the acoustic stimulation from the general electronic noise.

To confirm the effect of acoustic stimulation was not specific to sensors from a particular manufacturer, sensors from different manufacturers were stimulated with a 500 Hz sound wave. The Fourier transform results are given in SI Figures S4 and S5. For all sensors the Fourier transform of the baseline current shows a single constituent frequency. The frequency of this was consistent across all sensor types, hence the reported behaviour is not limited to a single sensor type or manufacturer.

There are several key findings from this analysis. (1) The RMS fluctuation and amplitude of the baseline current noise of an electrochemical gas sensor is amplified by acoustic stimulation; (2) The magnitude of this amplification depends on the proximity of the sensor to the source of sound; (3) The high frequency time series data for the baseline current can be decomposed into constituent frequencies, which depend on the frequency of the acoustic stimulation and the sampling rate; (4) A mixed sound can be decomposed into the individual sound frequencies that make up the mixture.

In addition to changing the frequency of the acoustic stimulation, the decibel level can also be varied. Changing the decibel level at the sensor will change the magnitude of the air pressure fluctuations at the interface. Two methods were used to accomplish this. The first involved changing the volume of the tone generator, and the second was to keep the volume fixed and change the proximity of the sensor to the sound source. The decibel level was recorded at the sensor. Time series data was recorded, and the Fourier transform results are given SI Figure S6. Figure 3A shows the magnitude of the frequency component corresponding to the imposed sound, determined by

the spectral analysis at different decibel levels. When the decibel level increases the magnitude of the acoustic frequency component increases. Data with a 1 Hz sampling rate was also recorded at different volumes (SI, Figure S7), and Figure 3B shows the calculated RMS variation versus dBA. The RMS variation also increased with increasing sound volume. Increasing the amplitude of the pressure fluctuations at the interface therefore increases the amplitude of the baseline current fluctuations, likely because the perturbations of the meniscus will be greater when the change in air pressure at the triple-phase interface is higher.

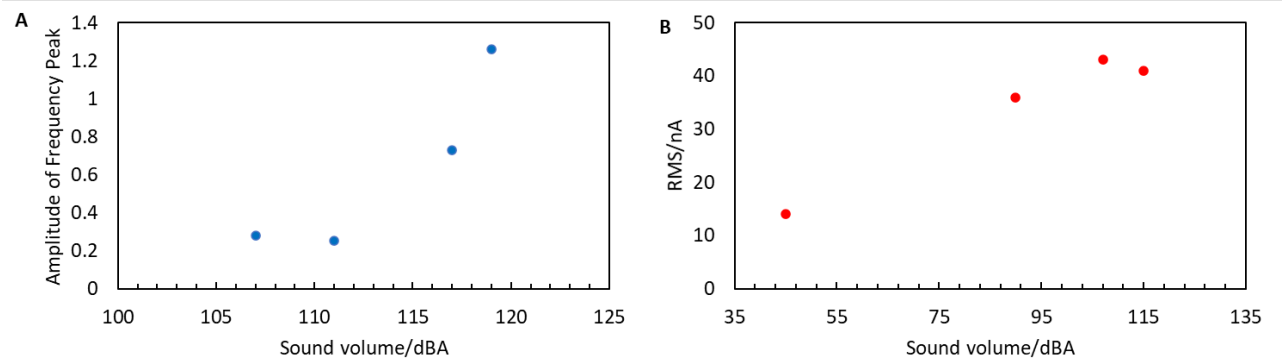

Figure 3: (A) Amplitude of the frequency component in the Fourier transform analysis of the O_3M5 current with increasing sound volume. Sampling rate of the time series data was 1 kHz. Sound wave frequency was 400 Hz. (B) RMS signal of the baseline current of an O_3M5 sensor with acoustic stimulation as a function of sound volume. Sampling rate of the time series data was 1 Hz. Sound wave frequency was 450 Hz.

We have shown that acoustic stimulation increases the magnitude of the baseline noise of an electrochemical sensor. The RMS variation of the 1 Hz data increased from 15 to 40 nA with acoustic stimulation, and fluctuations of up to 100 nA were seen. This would correspond to fluctuations of approximately 100 ppb, based on a sensitivity of -1000 nA ppm^{-1}. The sound levels we have studied are close to those found near urban roads. The amplitude and frequency of road traffic noise depends on traffic flow rate, vehicle speed, the road surface, and the proportion of heavy vehicles to cars. At a distance of 15 m, trucks typically give dBA levels between 75-95 dBA depending on the speed, and motorbikes in New Zealand are restricted to a maximum noise level of 100 dBA, while car horns typically have a noise level close to 110 dBA.[22-24] Spectra of road noise are dominated by low frequency bands below 2000 Hz. They typically show a component at approximately 100 Hz

caused by engine noise as well as a frequency peak around 1250 Hz due to the interaction of tyres with the road surface.[25-27]

Current data for an O_3M5 gas sensor was recorded at a sampling interval of 2 Hz over a 5-minute period in three different, real-world noise conditions: (1) indoors; (2) in a quiet area outdoors (approximately 200 m from the nearest road); (3) next to a busy road in an industrial part of Auckland, New Zealand. Figure 4 shows the current in these three situations. Additionally, two events are marked for the current recorded next to the road, which corresponded to times where large trucks drove past. The RMS variation of the current increased from 9 nA indoors, to 16 and 34 nA for the quiet and roadside outdoor tests respectively. Furthermore, fluctuations of approximately 80 nA (80 ppb equivalent) were seen when large trucks drove past. Figure 4 also shows the 10 second rolling RMS variation for the sensor next to the roadside. A clear increase in the RMS variation can be seen with the passage of large trucks. NO_2 concentrations range from approximately 10 to 100 ppb in ambient environments.[28-30] Whilst it is tempting to attribute the large current fluctuations when a truck passes to transient gas signals, the results presented above show that the effect of acoustic noise is an alternative and reasonable attribution. It is therefore reasonable to suggest that electrochemical gas sensors close to busy roads would be susceptible to baseline current fluctuations caused by nearby noise pollution that could mask the gas signal. Further, this could explain the increased noise during the day seen by various authors. The effect of sound cannot be isolated from gas concentration variations purely by measurement of the current hence if electrochemical sensors are used to deduce short time-scale fluctuations in gas concentration then effects of loud noise need to be considered.

Previous work studying the electrode impedance, for the sensors studied here [4] showed an effective electrode area of 1-6 m^2 and a Faradaic resistance, R_f , for the background electrochemical reactions in the absence of a target gas of approximately $1 – 6 \times 10^8$ Ω cm^2. The exchange current for the background electrode reactions is thus (*A* denoting area, *R* the gas constant, *T* the Kelvin

temperature and *z* the number of electrons per mole of reaction) $i_0 = ART/zFR_f \approx 10^{-6}$ A. A sound level of 120 dB corresponds to an root mean square pressure of 20 Pa or a peak pressure of ±28 Pa. The rms current fluctuation, i_{rms}, for this sound level is ~ 40 nA: that is, $i_{rms}/i_0 \approx 0.04$. For the purpose of consideration whether such a variation in current could be caused by such a small pressure oscillation, Figure 5 shows a highly simplified schematic representation of the sensor microstructure in which channels of electrolyte are pinned and confined onto the somewhat hydrophilic carbon electrode, within channels between the hydrophobic binder. This is similar to the model developed by Giner and Hunter [31]. The contact angle, θ, can be guessed based on the results of Gauthier et al. [32] : $\theta \approx 80^o$. The pressure difference, ΔP across the liquid interface would be :

$$\Delta P = \frac{2(1 - cos\theta)\gamma_{l,g}}{h} \approx \frac{0.35\gamma_{l,g}}{h} \tag{1}$$

where *h* (maximum value h_c) is the height of the cylindrical section of the fluid defined on Fig 5 and $\gamma_{l.g}$ is the interfacial tension between liquid and gas, ≈ 70 mN m^{-1} for the sulfuric acid electrolyte in air. If the pressure fluctuates (variations $\delta(\Delta P)$ then the only parameter in equation (1) that can change is the height, *h*, with changes δh given by:

$$\frac{\delta h}{h} = \frac{\delta(\Delta P)}{P} \tag{2}$$

If h_c (maximum value for *h*, defining the minimum value for ΔP) is small then ΔP will be large: for a channel with height 10 µm, $\Delta P \approx 2.5 \times 10^3$ Pa so the fluctuations in height caused by the sound pressure oscillations of 28 Pa would be small; $\delta h/h \approx 10^{-2}$. For larger channels on the other hand, with dimension ~ 100 µm, $\Delta P \approx 250$ Pa, so the fluctuations in height caused by the sound pressure would be significant; $\delta h/h \approx 10^{-1}$, which, based on the earlier work on meniscus electrochemistry cited above, would be sufficient to cause a relative change in current on the scale observed ($i_{rms}/i_0 \approx$ 0.04). Specifically, the change in shape of the gas-liquid boundary changes the boundary value

problem [19, 20] and hence the rate of diffusion-limited reactions, in this case the oxygen reduction contribution to the exchange current density. As shown by Ikesawa et al. [21], the oxygen reduction reaction current is dominated by that part of the electrode that is close to the gas-electrode-electrolyte contact line.

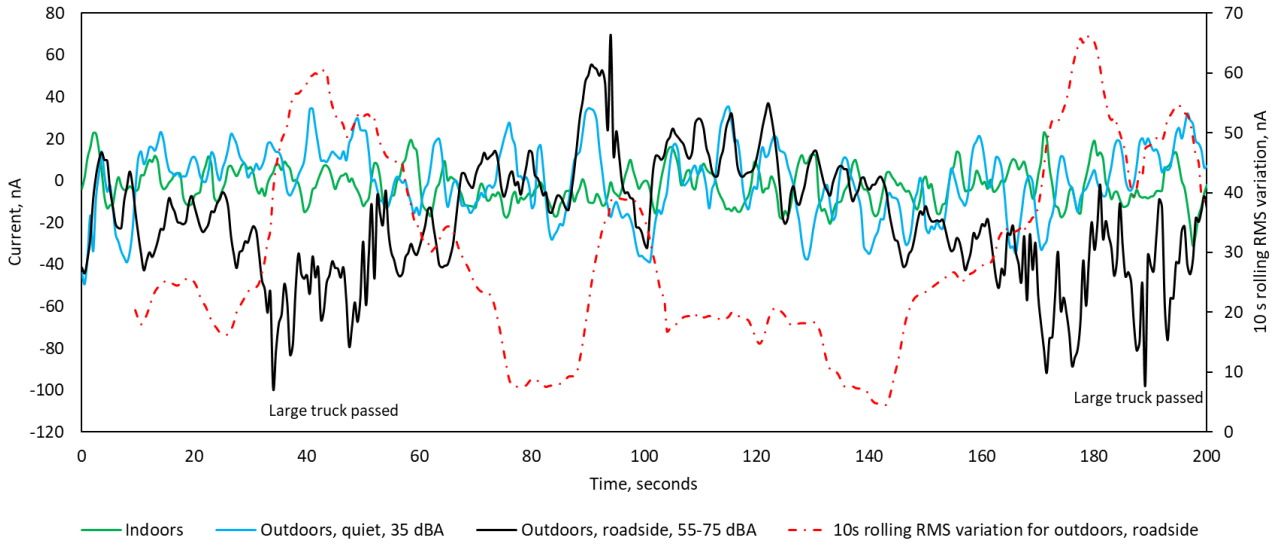

Figure 4: Current of an O_3M5 sensor in different sound settings: green = indoors, blue = quiet area outdoors (35 dBA), black = next to a busy road (55-75 dBA). Current collected at a sampling rate of 2 Hz. Two time periods where large trucks passed by are indicated. Also shown is the 10 second rolling RMS variation of the current collected next to the roadside.

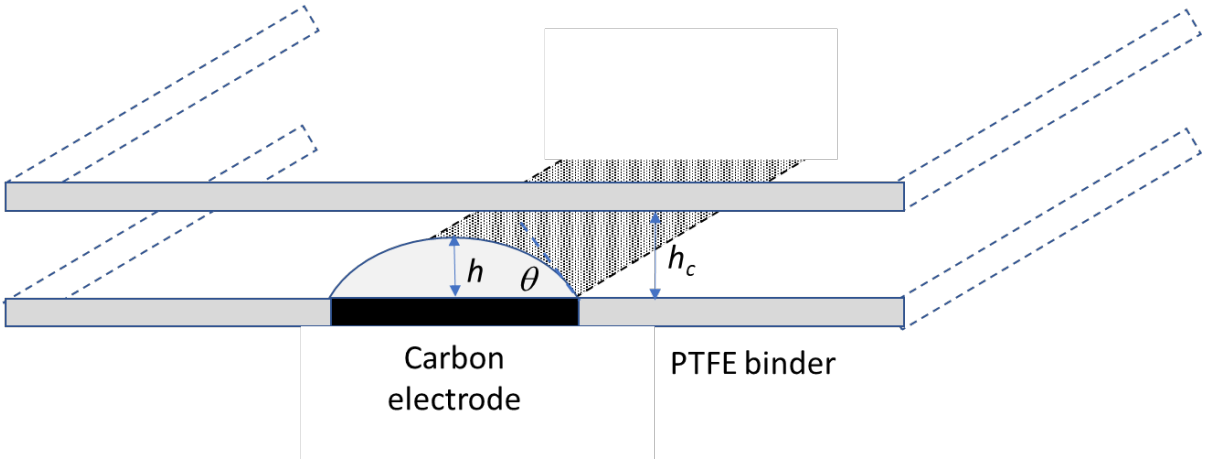

Figure 5: Schematic and idealised representation of the sensor microstructure used to assess the effects of pressure fluctuations. The electrolyte, contact angle θ, pinned at the boundary between the electrode and support material, is confined within channels of height h_c

Conclusion

We have demonstrated that electrochemical gas sensors, designed to measure the concentration of gaseous compounds, respond to acoustic stimulation. The RMS variation of the baseline current of various electrochemical sensors increases with acoustic stimulation and fluctuations of up to 100 ppb equivalent are seen in the 1 Hz data in response to loud sound. Fourier transform analysis of the baseline current when stimulated with a soundwave of fixed frequency shows that the baseline current fluctuations are composed of a single dominant frequency. The frequency of the baseline noise follows the frequency of the applied sound. The amplitude of the baseline fluctuations, shown by both the magnitude of the constituent frequency peak in the Fourier transform analysis and the RMS signal of the baseline current at low sampling rate, depends on the amplitude of the applied sound. We hypothesize that this effect is caused by air pressure fluctuations at the three-phase interface of the electrochemical gas sensor. These could mechanically perturb the shape, area, and contact angle of the meniscus, resulting in fluctuations in the oxygen reduction and electrode oxidation current at the working electrode, which manifests as amplification of the baseline noise. We use an idealised model to illustrate that the effect would be dominated by the largest pores within the porous composite electrode structure. As noted previously, acoustic or Helmholtz resonance, which is caused by the passage of wind across the external orifice of the sensor, would also cause variations in air pressure at the triple-phase boundary.[2] Further work is needed to evaluate the impact of pressure fluctuations caused by acoustic resonance on the baseline current reactions of electrochemical gas sensors. The frequency response has not been studied, but the expectation is that, since the sensor acts as a series RC element [4], the acoustic signal would fall off with increasing frequency dependent on the interfacial capacitance and electrolyte resistance.

References

1. Baron, R. and J. Saffell, *Amperometric gas sensors as a low cost emerging technology platform for air quality monitoring applications: A review.* ACS Sensors, 2017. **2**(11): p. 1553-1566.
2. Williams, D.E., *Electrochemical sensors for environmental gas analysis.* Current Opinion in Electrochemistry, 2020. **22**: p. 145-153.
3. Bibic, D., et al., *NEW APPROACH OF MEASURING TOXIC GASES CONCENTRATIONS: APPLICATION EXAMPLES.* Annals of DAAAM & Proceedings, 2018. **29**.
4. Farquhar, A.K., G.S. Henshaw, and D.E. Williams, *Understanding and Correcting Unwanted Influences on the Signal from Electrochemical Gas Sensors.* ACS sensors, 2021. **6**(3): p. 1295-1304.
5. Hitchman, M.L. and J.R. Saffell, *Considerations of thermodynamics and kinetics for the effects of relative humidity on the electrolyte in electrochemical toxic gas sensors.* ACS sensors, 2021. **6**(11): p. 3985-3993.
6. Mead, M., et al., *The use of electrochemical sensors for monitoring urban air quality in low-cost, high-density networks.* Atmospheric Environment, 2013. **70**: p. 186-203.
7. Jiao, W., et al., *Community Air Sensor Network (CAIRSENSE) project: evaluation of low-cost sensor performance in a suburban environment in the southeastern United States.* Atmospheric Measurement Techniques, 2016. **9**(11): p. 5281-5292.
8. Duvall, R.M., et al., *Performance evaluation and community application of low-cost sensors for ozone and nitrogen dioxide.* Sensors, 2016. **16**(10): p. 1698.
9. Liang, Y., et al., *Field comparison of electrochemical gas sensor data correction algorithms for ambient air measurements.* Sensors and Actuators B: Chemical, 2021. **327**: p. 128897 DOI 10.1016/j.snb.2020.128897.
10. Masson, N., R. Piedrahita, and M. Hannigan, *Quantification Method for Electrolytic Sensors in Long-Term Monitoring of Ambient Air Quality.* Sensors, 2015. **15**(10): p. 27283-27302.
11. Popoola, O.A., et al., *Development of a baseline-temperature correction methodology for electrochemical sensors and its implications for long-term stability.* Atmospheric Environment, 2016. **147**: p. 330-343.
12. Pang, X., et al., *The impacts of water vapour and co-pollutants on the performance of electrochemical gas sensors used for air quality monitoring.* Sensors and Actuators B: Chemical, 2018. **266**: p. 674-684.
13. Ouyang, B., *First-Principles Algorithm for Air Quality Electrochemical Gas Sensors.* ACS Sensors, 2020. **5**(9): p. 2742-2746.
14. Pang, X., et al., *Electrochemical ozone sensors: A miniaturised alternative for ozone measurements in laboratory experiments and air-quality monitoring.* Sensors and Actuators B: Chemical, 2017. **240**: p. 829-837.
15. Weissert, L., et al., *Low-cost sensors and microscale land use regression: Data fusion to resolve air quality variations with high spatial and temporal resolution.* Atmospheric Environment, 2019. **213**: p. 285-295.
16. Sedlák, P., P. Kuberský, and F. Mívalt, *Effect of various flow rate on current fluctuations of amperometric gas sensors.* Sensors and Actuators B: Chemical, 2019. **283**: p. 321-328.
17. Maget, H. and R. Roethlein, *The Electrochemical Reduction of Oxygen on Platinum Electrodes Partially Immersed in Sulfuric Acid.* Journal of The Electrochemical Society, 1965. **112**(10): p. 1034-1040.
18. Chan, K.-Y., J.F. Cocchetto, and G.S. Efthymiou, *Meniscus behavior and oxygen reduction in tapered pore gas diffusion electrodes.* Electrochimica acta, 1988. **33**(12): p. 1767-1773.
19. Braide-Azikiwe, D.C.B., et al., *Soap film electrochemistry.* Electrochemistry Communications, 2009. **11**(6): p. 1226-1229.

20. Vannoy, K.J., et al., *Detecting Methamphetamine in Aerosols by Electroanalysis in a Soap Bubble Wall.* Analytical Chemistry, 2022. **94**(16): p. 6311-6317.
21. Ikezawa, A., et al., *Direct measurements of local current distributions on electrodes covered with thin liquid electrolyte films.* Electrochemistry Communications, 2017. **84**: p. 53-56.
22. CDC. *Centers for Disease Control and Prevention: What Noises Cause Hearing Loss*. 2019 14/10/2021]; Available from: https://www.cdc.gov/nceh/hearing_loss/what_noises_cause_hearing_loss.html#:~:text=Sound%20is%20measured%20in%20decibels,immediate%20harm%20to%20your%20ears.
23. Waka Kotahi, N.Z. *NZ Transport Agency: Noise tests for exhausts*. 2021 21/10/2021]; Available from: https://www.nzta.govt.nz/vehicles/warrants-and-certificates/warrant-of-fitness/noise-tests-for-exhausts/.
24. Close, W. and J. Wesler, *Vehicle noise sources and noise-suppression potential.* Motor Vehicle Noise Control, 1975.
25. Pearse, J., *Road Traffic and Aircraft Noise Spectrums*. 2011, University of Canterbury.
26. Can, A., et al., *Traffic noise spectrum analysis: Dynamic modeling vs. experimental observations.* Applied Acoustics, 2010. **71**(8): p. 764-770.
27. Torija, A.J., et al., *Relationship between road and railway noise annoyance and overall indoor sound exposure.* Transportation research part D: transport and environment, 2011. **16**(1): p. 15-22.
28. Keuken, M., M. Roemer, and S. van den Elshout, *Trend analysis of urban NO2 concentrations and the importance of direct NO2 emissions versus ozone/NOx equilibrium.* Atmospheric Environment, 2009. **43**(31): p. 4780-4783.
29. Lee, H.J. and P. Koutrakis, *Daily ambient NO2 concentration predictions using satellite ozone monitoring instrument NO2 data and land use regression.* Environmental science & technology, 2014. **48**(4): p. 2305-2311.
30. Lin, C., et al., *Evaluation and calibration of Aeroqual series 500 portable gas sensors for accurate measurement of ambient ozone and nitrogen dioxide.* Atmospheric Environment, 2015. **100**: p. 111-116.
31. Giner, J. and C. Hunter, *The Mechanism of Operation of the Teflon-Bonded Gas Diffusion Electrode: A Mathematical Model.* Journal of The Electrochemical Society, 1969. **116**(8): p. 1124-1130.
32. Gauthier, E., et al., *Drop Detachment and Motion on Fuel Cell Electrode Materials.* Acs Applied Materials & Interfaces, 2012. **4**(2): p. 761-771.